

Q effects on thin-bed AVO/AVF analysis

Wenyong Pan*, Kris Innanen
CREWES, University of Calgary
wpan@ucalgary.ca

Summary

Zoeppritz equations are the bases for traditional AVO analysis, which plays a significant role in oil and gas exploration. They are not however suitable for quantitative analysis of the amplitude response of thin-beds. In this paper, we analyzed the Q effects on thin-bed AVO/AVF responses in a dispersive system. Several interesting conclusions have been drawn. (1) If the thin-bed thickness and Q are both fixed, with increasing frequency, the Q effects on reflections R_{PP} (real parts) become stronger, while the Q effects on reflections R_{PS} (real parts) become weaker; (2) when the frequency and thin-bed thickness are fixed, with decreasing Q, the Q effects on both R_{PP} and R_{PS} become stronger; and (3), when the frequency and Q are fixed, the Q effects on the real parts of both R_{PP} and R_{PS} become stronger with thin-bed thinning. And Q also influences the imaginary parts of R_{PP} and R_{PS} , but these effects are weaker.

Introduction

In amplitude-variation-with-offset (AVO) techniques, seismic reflection amplitudes are analyzed to facilitate hydrocarbon detection (Castagna and Backus, 1993; Aki and Richards, 2002). Traditional AVO techniques rely primarily on the Zoeppritz equations and their solutions and they describe the transmission and reflection when plane wave impinging upon one single interface which separates two infinite half spaces. However, the Zoeppritz equations do not permit quantitative interpretation of the amplitude response of thin beds. Because as a geological layer thins, the reflections from the top and bottom interfaces overlap, and the resulting wave is significantly different from that due to a single interface.

Thin-bed AVO has been considered from many different points of view in recent decades. Widess (1973) studied the reflections from the top and bottom interfaces of a thin layer at normal incidence. Chung and Lawton (1995) derived two analytical expressions for the normal incidence amplitude response, as a function of the bed thickness. Liu and Schmitt (2003) derived an exact analytical solution to model the reflection amplitude at full incidence and analyzed the AVO responses of thin-bed within acoustic regime. Pan and Innanen (2013) extended thin-bed AVO/AVF analysis from acoustic media to elastic media and discussed the amplitude responses with varying incident angle, thin-bed thickness and frequency. The AVF response of dispersive targets has more recently drawn significant attention also (e.g., Odebeatu et al., 2006; Quintal et al., 2009; Innanen, 2011; Lines et al. 2012). This research made a further extension by taking Q into consideration to analyze the thin-bed AVO/AVF responses. And it is possible for us to analyze the changes of the real and imaginary parts of the amplitude with varying frequency, incident angle and thin-bed thickness.

Theory and Method

Figure 1 shows the single interface model used in traditional AVO analysis. The geometrical configuration for thin-bed AVO analysis is illustrated in Figure 2. The thin-bed (layer 2) is embedded between two infinite half spaces. A plane harmonic and compressional wave (P-wave) impinges on

interface 1, causing both a reflected P-wave and a reflected (converted) shear wave (S-wave), as well as a transmitted P-wave and S-wave. The transmitted P-wave and S-wave produce multiple reflections within layer 2. The total wave response involves overlapping reflected and transmitted waves at point C in Figure 2. This renders the Zoeppritz equations unsuitable as a tool for analysis of the upgoing field due to interface 1. In Figure 2, z is the thickness of thin-bed (layer 2). In this research, we use $n=\lambda/z$ to analyze the AVO responses when varying z , where λ is the dominant wavelength.

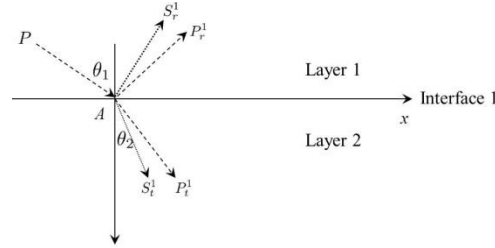


Figure 1: Single interface model for traditional AVO analysis.

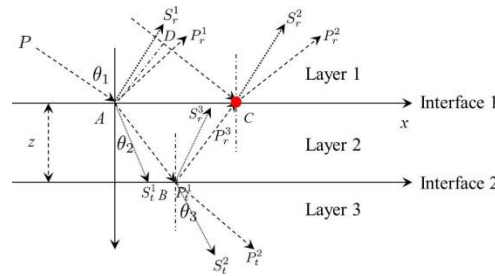


Figure 2: Three-layer model used for thin-bed AVO analysis (Pan and Innanen, 2013).

We simplify the layered elastic medium theory due to Brekhovskikh (1993), to coincide with three-layer elastic media. The displacements and stresses in layer 1 and layer 3 are connected by one coefficient matrix C , as shown in equation (1). Each element in matrix C has been listed in Pan (2012). And for computational convenience, we assume that layer 1 and layer 3 have the same elastic properties. Hence, we have

$$\begin{bmatrix} u_x^3 \\ u_z^3 \\ \sigma_{zz}^3 \\ \tau_{zx}^3 \end{bmatrix} = C \begin{bmatrix} u_x^1 \\ u_z^1 \\ \sigma_{zz}^1 \\ \tau_{zx}^1 \end{bmatrix} = \begin{bmatrix} C_{11} & C_{12} & C_{13} & C_{14} \\ C_{21} & C_{22} & C_{23} & C_{24} \\ C_{31} & C_{32} & C_{33} & C_{34} \\ C_{41} & C_{42} & C_{34} & C_{44} \end{bmatrix} \begin{bmatrix} u_x^1 \\ u_z^1 \\ \sigma_{zz}^1 \\ \tau_{zx}^1 \end{bmatrix}, \quad (1)$$

where $u_x^1, u_z^1, \sigma_{zz}^1, \tau_{zx}^1, u_x^3, u_z^3, \sigma_{zz}^3,$ and τ_{zx}^3 represent the displacements and stresses in layers 1 and 3 respectively. Using these quantities we obtain:

$$VR = X, \quad (2)$$

where $R = (R_{PP} \ R_{PS} \ T_{PP} \ R_{PS})^T, V = (V_1 \ V_2 \ V_3 \ V_4)$. And matrix X and each column in matrix V can be expressed using matrix C (Pan, 2012). According to Cramer's rule, we can obtain four matrices $V_{PP}, V_{PS}, V'_{PP}, V'_{PS}$, by replacing the first, the second, the third and then the fourth columns for matrix V with X . The elements of V and X are listed in Appendix A of Pan and Innanen (2013). We then express reflection and transmission coefficient as follows:

$$R_{PP}(\theta, \omega, z) = \frac{\det V_{PP}}{\det V}, R_{PS}(\theta, \omega, z) = \frac{\det V_{PS}}{\det V}, T_{PP}(\theta, \omega, z) = \frac{\det V'_{PP}}{\det V}, T_{PS}(\theta, \omega, z) = \frac{\det V'_{PS}}{\det V}, \quad (3)$$

To study the amplitude response of thin-bed in anelastic media by taking Q into consideration, standard NCQ models (Aki and Richards, 2002; Innanen, 2012) are framed in terms of the propagation constants:

$$k_P = \frac{\omega}{V_P} [1 + Q_P^{-1} F_P(\omega)], k_S = \frac{\omega}{V_S} [1 + Q_S^{-1} F_S(\omega)], \quad (4)$$

where following ‘anacoustic’ scattering theory (Innanen and Weglein, 2007) we have sequestered the attenuation and dispersion terms in the functions:

$$F_P(\omega) = \frac{i}{2} - \frac{1}{\pi} \log\left(\frac{\omega}{\omega_P}\right), F_S(\omega) = \frac{i}{2} - \frac{1}{\pi} \log\left(\frac{\omega}{\omega_S}\right), \quad (5)$$

And equation (4) implies:

$$\tilde{V}_P = V_P [1 + Q_P^{-1} F_P(\omega)]^{-1}, \tilde{V}_S = V_S [1 + Q_S^{-1} F_S(\omega)]^{-1}, \quad (6)$$

Examples

Table.1 shows the elastic parameters used for amplitude response analysis. Layer 1 and layer 3 are both shale with the same elastic parameters and layer 2 indicating thin-bed is gas sand. Firstly, we fixed the thin-bed thickness z at $\lambda/4$ ($n=4$) and fixed Q at 10, while varied the frequency from 10Hz to 80Hz with a step of 10Hz. The real parts of R_{PP} and R_{PS} AVO curves are shown in Figure 3a and b respectively. The black, red, blue, green, cyan, brown, pink and gray lines indicate the AVO curves when the frequency f is 10Hz, 20Hz, 30Hz, 40Hz, 50Hz, 60Hz, 70Hz and 80Hz respectively. And the bold black lines are the AVO curves without attenuation. We can observe that the R_{PP} AVO curves depart the AVO curve without attenuation with increasing frequency, while R_{PS} AVO curves approach the AVO curve without attenuation. This means that with increasing frequency, the Q effects on reflections R_{PP} (real parts) become stronger, while the Q effects on reflections R_{PS} (real parts) become weaker.

Table 1: Elastic parameters of the thin-bed model (gas bearing thin bed model)

Model	Rock Type	α (m/s)	β (m/s)	α/β	ρ (g/cm ³)	σ
Layer 1	Shale	2850	1053	2.23	2.2	0.1
Layer 2	Gas Sand	2900	1933	1.67	2.3	0.4
Layer 3	Shale	2850	1053	2.23	2.2	0.1

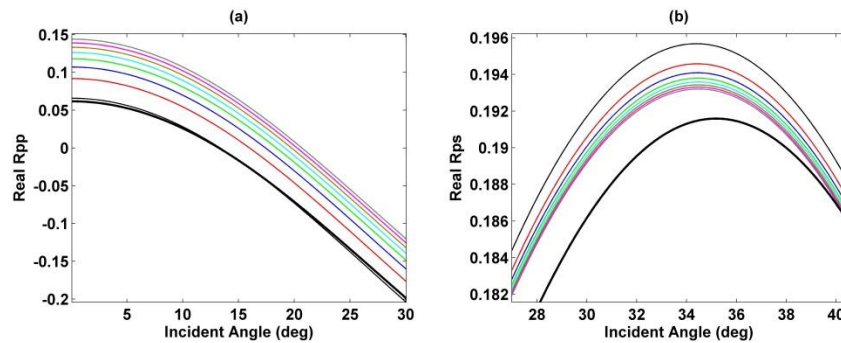


Figure 3: Real R_{PP} (a) and R_{PS} (b) when $n=4$ and $Q=10$ while varying frequency from 10Hz to 80 Hz with a step of 10 Hz.

Then, we compared the real parts of R_{PP} and R_{PS} reflections with changing Q ($Q=Q_P=Q_S$) among 10, 20, 30, 40, 50 and 90 indicated by magenta, red, blue, cyan and black lines and varying the thin-bed thickness among $n=4$ (Figure 4a and b), $n=10$ (Figure 4c and d), $n=40$ (Figure 4e and f) and $n=80$ (Figure 4g and h). We can see that with increasing Q , the AVO curves of real R_{PP} and R_{PS} approach those with no attenuation (the bold-black lines) as expected. Another thing we can observe is that with the thin-bed thinning, the Q effects on both R_{PP} and R_{PS} become stronger.

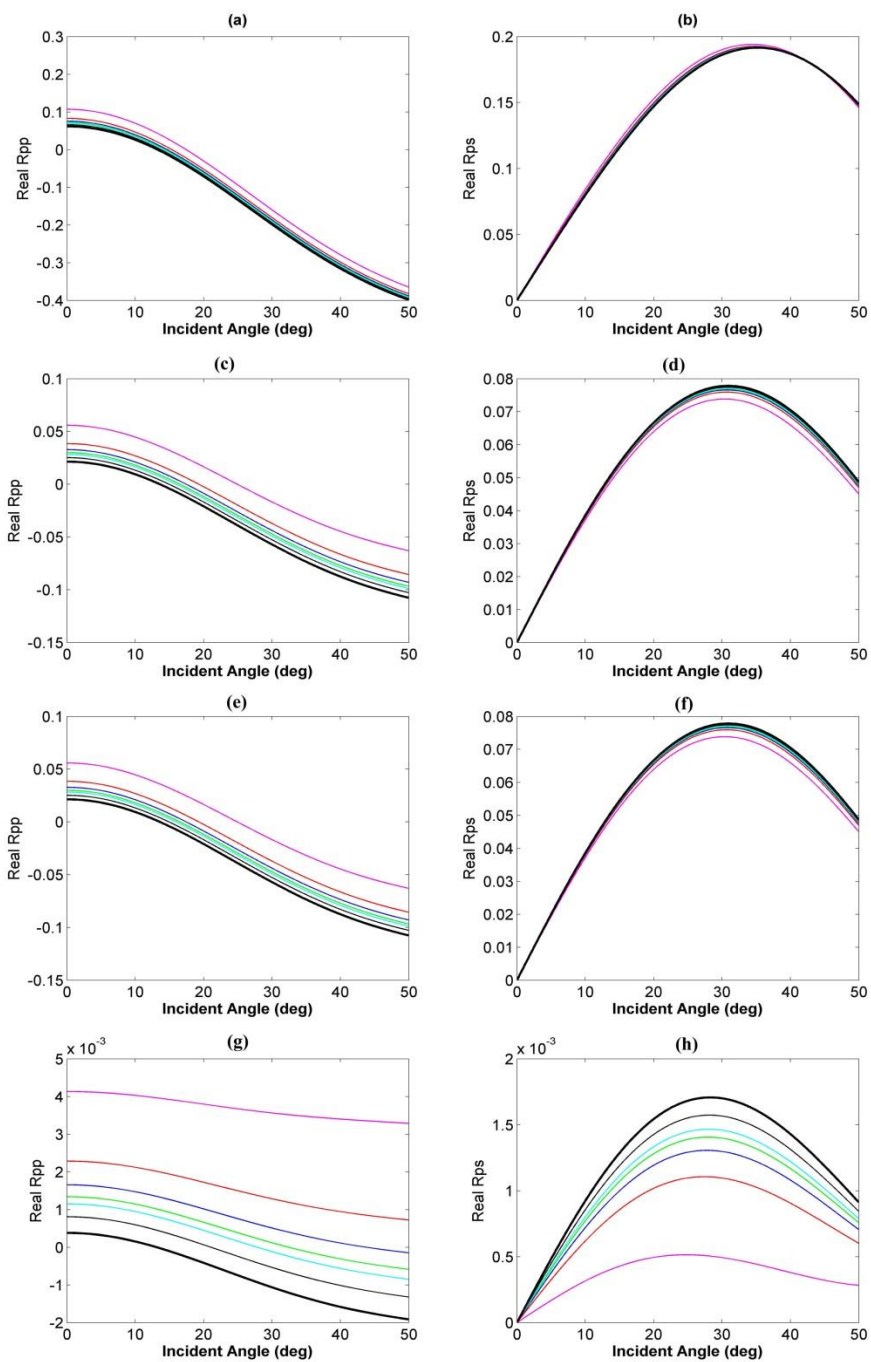


Figure 4: (a), (c), (e) and (g) show the real R_{PP} when frequency $f=30\text{Hz}$ and $n=4, 10, 40$ and 80 respectively. (b), (d), (f) and (h) show the real R_{PS} when $n=4, 10, 40$ and 80 respectively.

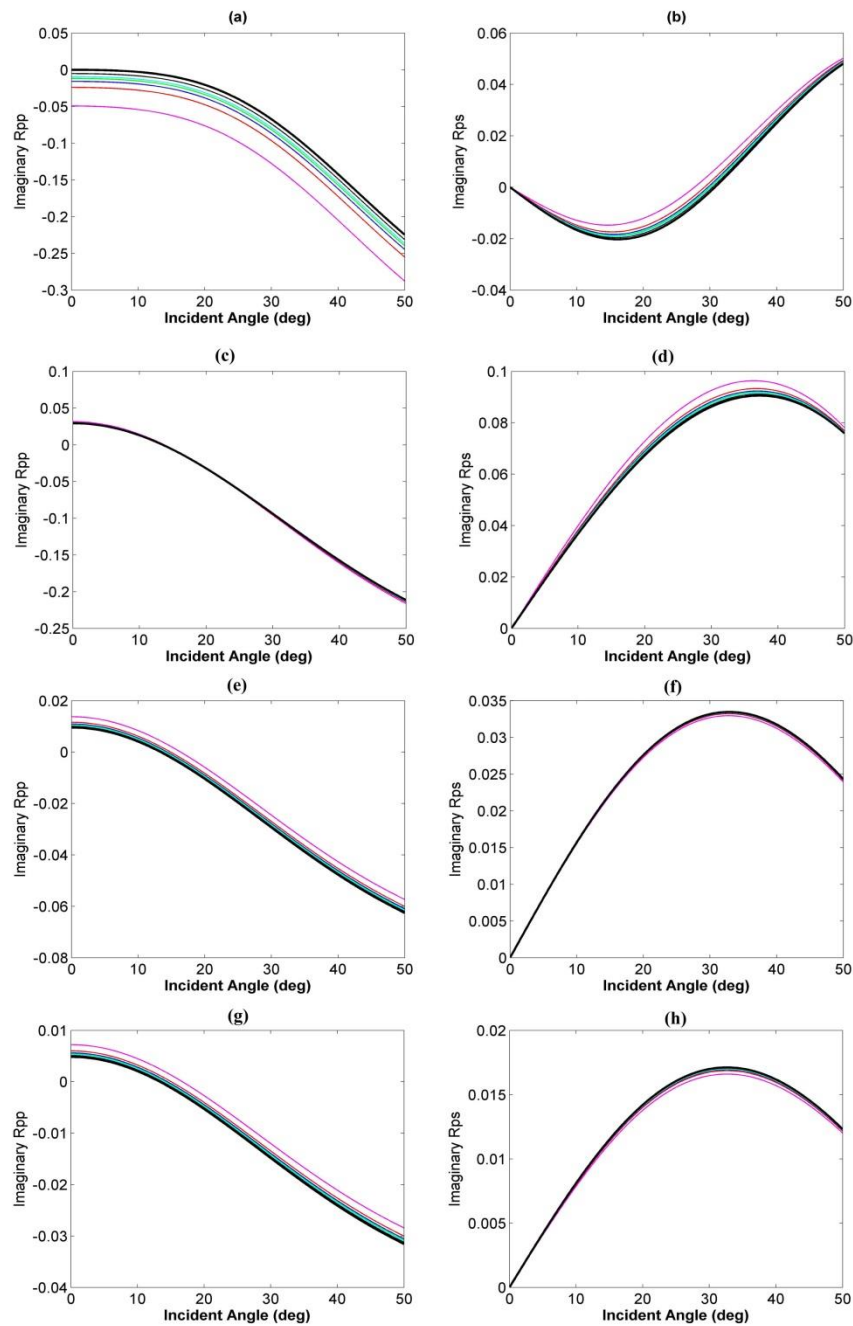


Figure 5: (a), (c), (e) and (g) show the imaginary R_{PP} when frequency $f=30\text{Hz}$ and $n=4, 10, 40$ and 80 respectively. (b), (d), (f) and (h) show the imaginary R_{PS} when $n=4, 10, 40$ and 80 respectively.

We also analyzed the Q effects on the imaginary parts of R_{PP} and R_{PS} when thin-bed thickness is $n=4$ (Figure 5a and b), $n=10$ (Figure 5c and d), $n=40$ (Figure 5e and f) and $n=80$ (Figure 5g and h). It can be seen that the Q can also produce influence on imaginary parts of R_{PP} and R_{PS} but the effects are weaker than those on real parts of R_{PP} and R_{PS} . We can also notice that the Q effects on imaginary R_{PP} become weaker and then stronger. When $n=10$, the Q effects are not obvious to observe.

Conclusions

According to the discussion and analysis above, several interesting conclusions can be achieved: Q can produce obvious influences on R_{PP} and R_{PS} for thin-bed AVO/AVF analysis. If the thin-bed thickness and Q are both fixed, with increasing frequency, the Q effects reflections R_{PP} (real parts) become stronger, while the Q effects on reflections R_{PS} (real parts) become weaker. When the frequency and thin-bed thickness are fixed, with decreasing Q , the Q effects on both R_{PP} and R_{PS} become stronger. Furthermore, Q can also produce influence on the real parts and imaginary parts of R_{PP} and R_{PS} .

Acknowledgements

This research was supported by the Consortium for Research in Consortium of Elastic Wave Exploration Seismology (CREWES).

References

- Aki, K., and Richards, P. G., 2002, Quantitative Seismology: University Science Books, 2nd edn.
- Brekhovskikh, L. M., 1960, Wave in layered media: Academic Press.
- Castagna, J. P. and M. Backus, 1993, Offset-dependent reflectivity: theory and practice of AVO analysis: SEG.
- Lines, L., Innanen, K.A., Vasheghani, F., Wong, J., Sondergeld, C., Treitel, S., and Ulrych, T., 2012, Experimental Confirmation of "Reflections on Q ": SEG Expanded Abstracts, 1–5.
- Liu, Y., and Schmitt, D.R., 2003, Amplitude and AVO responses of a single thin bed: Geophysics, **68**, 1161–1168.
- Innanen, K. A., 2011, Inversion of the seismic AVF/AVA signatures of highly attenuative targets: Geophysics, **76**, R1–R11.
- Odebeatu, E., J. Zhang, M. Chapman, E. Liu, and X.-Y. Li, 2006, Application of spectral decomposition to detection of dispersion anomalies associated with gas saturation: The Leading Edge, **25**, 206–210.
- Pan, W., and Innanen, K.A., 2013, AVO/AVF analysis of thin-bed in elastic media: SEG Expanded Abstracts, 373–377.
- Pan, W., 2012, AVO/AVF analysis of thin-bed in elastic media: CREWES Research Report.
- Quintal, B., S.M. Schmalholz, and Y. Y. Podladchikov, 2009, Low-frequency reflections from a thin layer with high attenuation caused by interlayer flow: Geophysics, **74**, no. 1, N15–N23.
- Widess, M.B., 1973, How thin is a thin bed? : Geophysics, **38**, 1176–1180.